SUPPLEMENTARY INFORMATION

Surface-Enhanced Nitrate Photolysis on Ice.

Guillaume Marcotte, Patrick Marchand, Stéphanie Pronovost, Patrick Ayotte*

Département de chimie,
Université de Sherbrooke,
2500, boul. de l'Université,
Sherbrooke (Québec)
Canada J1K 2R1

Carine Laffon and Philippe Parent*

CINaM-CNRS
Campus de Luminy Case 913
13288 Marseille,
France

*Corresponding authors:
Patrick.Ayotte@USherbrooke.ca; Tel.: 1-819-821-7889;
parent@cinam.univ-mrs.fr; Tel.: 33 (0)6 60 30 28 07.

I. Kinetic modeling of the photochemical NO_2 emissions from ice to the snowpack interstitial air.

A simple 1D kinetic model was elaborated to study the effects of enhanced heterogeneous nitrates photolysis on NO_2 emissions from ice to the snowpack interstitial air at 243 K based on the simplified kinetic scheme illustrated in Figure S1. While most models describe snow-bound impurities, and their (photo)chemistry, as occurring essentially exclusively in a superficial QLL,[1,2] this model assumes nitrates concentrations (4.4μM)[3] to be homogeneously distributed throughout the bulk. A kinetic master equation describes the photolysis of NO_3^-:

$$NO_3^- \xrightarrow{h\nu} NO_2 + O^- \qquad \text{(R1)}$$

and the hydrolysis of NO_2:

$$NO_2 + NO_2 + H_2O \xrightarrow{\Delta} H^+ + {NO_3}^- + HONO \qquad \text{(R2)}$$

within each individual layer. While *bulk* photolysis[4] and *bulk* hydrolysis rate constants are assigned to layers 2 to 3000, *surface-specific* rate constants could be assigned to layer 1 allowing to account for *enhanced* heterogeneous hydrolysis[5–7] and *enhanced* heterogeneous photolysis [i.e., the effects of a 3x(6x) enhancement over bulk nitrates photolysis rates from Galbavy et al.[4] were investigated] in the single, top-most surface layer on ice. The effect of diurnal cycles in the actinic flux is modeled by modulating the nitrates photolysis rates.[8]

Diffusive transport kinetics for NO_3^- and NO_2 between adjacent layers within bulk ice (layers 2 to 3000) as well as with its surface layer (layer 1) are described explicitly using 1-D fickian diffusion. The much faster kinetics for NO_2 adsorption onto, and desorption from the surface layer:

$$NO_{2(g)} \overset{K_{ads}}{\longleftrightarrow} NO_{2(ads)} \qquad \text{(R3)}$$

couple the condensed phase processes with the gas phase are described using an equilibrium partition coefficient.[9] Finally, the kinetic master equation was numerically integrated over the diurnal cycles in the actinic flux using a 3.6 s time-step. Identical results were obtained using a 3.6 ms time-step in a few shorter simulations.

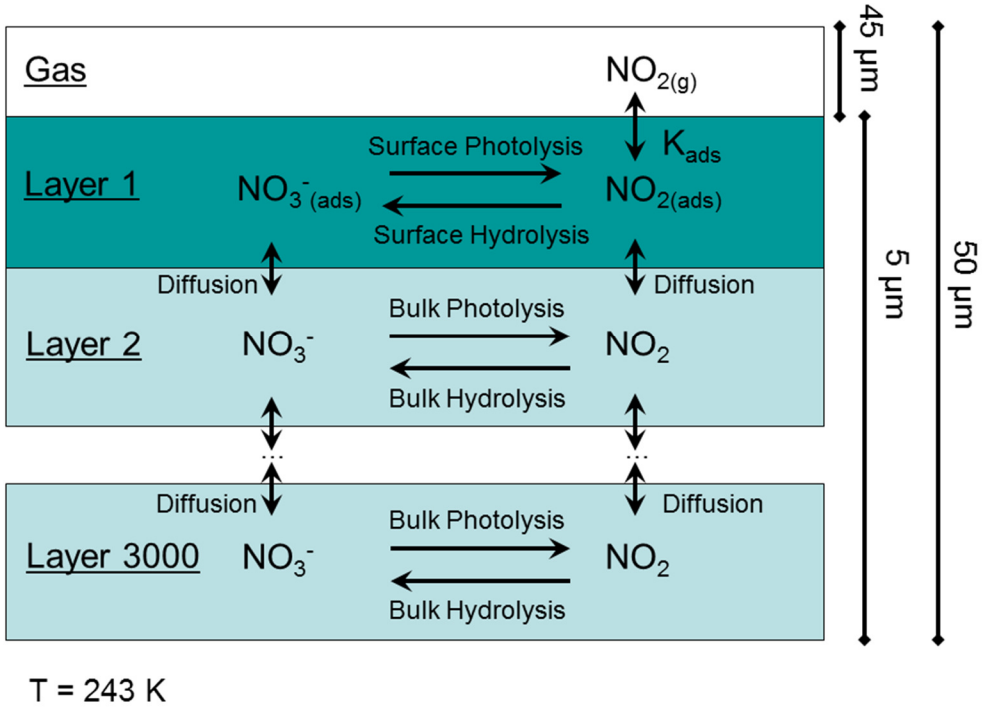

Fig. S1. Schematics of the kinetic scheme used to describe the contribution of enhanced nitrate photolysis rates at the surface of ice to the photochemical NO_2 emissions to the snowpack interstitial air at 243 K.

It is important to stress that this simplified kinetic model is not intended to reproduce neither the (photo)chemical NO_x fluxes nor the interstitial air or polar boundary layer NO_2 mixing ratios observed in the field. Rather, its goal is to evaluate the magnitude of the contribution from enhanced photolysis of nitrates adsorbed onto the topmost layer on ice to the NO_2 mixing ratio in the snowpack interstitial air on a typical windless summer day at the polar boundary layer. As a point of reference, it was chosen to relate, where applicable, to observations from field studies by Dibb et al.[10] at Summit, Greenland, and by Frey et al.[11] at Dome Concordia, Antarctica. For instance, these reports describe modulations in the amplitude of NO_x (i.e., NO, NO_2 and HONO) mixing ratios and their characteristic response time to abrupt changes in UV irradiance. Of particular relevance to this work, Dibb et al.[10] reported that the NO_2 photochemical fluxes can be modulated (i.e., turned on and off by blocking the actinic flux) on a timescale shorter than 8 minutes (i.e., the resolution of their field data). Given the slow molecular transport kinetics in ice, this suggests that most of the NO_2 emissions must originate from the near-surface region of the ice within the snowpack. These field observations therefore provided qualitative guidelines to set lower bounds in the heterogeneous NO_2 hydrolysis while also providing upper bounds for the bulk NO_2 diffusion/NO_2 hydrolysis rates that should be used to describe these complex coupled (photo)chemical processes within ice crystals and at their surface. The kinetic parameters used in the model are summarized in Table S1.

Table S1: Kinetic parameters used in the model

Parameter	Value (Reference)	Comment
$D_{NO_3^-}$	2.5x10^{-15} m^{2}s^{-1} (12)	Calculated at 243 K using kinetic parameters reported by Thibert and Dominé.[12]
D_{NO_2}	2.4x10^{-14} m^{2}s^{-1} (13)	Approximated using data for CO_2 in ice cores at 248 K from Bereiter et al.[13]
$J^{Bulk}_{NO_3^- photolysis}$	2.2x10^{-7} s^{-1} (4)	Nitrates photolysis rate measured in the field by Galvaby et al.[4] using 1 mM frozen aqueous solutions in borosilicate NMR tubes buried at a depth of 15 cm within the snowpack at a temperature of ~253 K were interpreted as bulk nitrates photolysis rates.
$J^{Surface}_{NO_3^- photolysis}$	2.2x10^{-7} s^{-1} (4) 0.65(1.3)x10^{-6} s^{-1}	Nitrates photolysis rates in the surface layer were either considered the same as that of bulk nitrates (top entry, ref 4), or were enhanced 3(6)-fold with respect to the bulk nitrates photolysis rates (bottom entry, this work).
K_{ads}	2.3 x10^{-3} (9)	The gas/surface partition coefficient for NO_2 on ice was calculated for the surface to volume ratio of the model using data reported by Bartels-Rauch et al.[9] for adsorption of NO_2 on crystalline ice at 246 K.
$k^{Bulk}_{NO_2 hydrolysis}$	1.5x10^4 M^{-1}s^{-1} (13,14)	Bulk NO_2 hydrolysis rates in ice were considered diffusion-limited and calculated using the diffusion coefficient for CO_2 in ice from Bereiter et al.[13] For comparison, the corresponding rate constant for NO_2 hydrolysis in aqueous solutions at 293 K was reported to be 2.2x10^7 M^{-1}s^{-1} by Cheung et al.[14]
$k^{Surface}_{NO_2 hydrolysis}$	1.7x10^{-4} pptv^{-1}s^{-1} (6)	Heterogeneous NO_2 hydrolysis rates were considered to be first order in gas phase $NO_{2(g)}$ and first order in NO_2 adsorbed onto the first layer on ice, $NO_{2(ads)}$. Rates were adapted from Svensson et al.[6] using kinetic gas theory to calculate an effective heterogeneous hydrolysis rate constant at 243 K. Considering the reaction to be second order in $NO_{2(ads)}$, the NO_2 hydrolysis rate constant on ice is enhanced ~10^6-fold with respect to the bulk in the model. For comparison, heterogeneous NO_2 hydrolysis was reported to be enhanced by as much as ~10^5 at wet surfaces compared to bulk liquid water by Finlayson-Pitts et al.[7]

I.A Snow microstructure and initial concentration profiles:

The physical dimensions used in the 1-D kinetic model are based on a mean snow crystal thickness of 10 μm and a snow porosity of 90%, in agreement with morphological parameters typical of fresh snow.[15] The bulk transport kinetics are discretized using 3000 layers having a thickness of 1.67 nm (i.e., corresponding to ~4.5 ice bilayers) and periodic boundary conditions are imposed (i.e., along the vertical axis of Figure S1). While both nitrates photolysis and NO_2 hydrolysis occur in bulk ice (Section I.B), they are much more efficient in the surface layer (Section I.C). Kinetic parameters describing these processes in the surface layer were thus assigned different values than those occurring in the 2999 bulk layers (see Table S1). Interstitial air $NO_{2(g)}$ mixing ratio and bulk concentrations were initially set to zero. A homogeneous initial bulk NO_3^- concentration of 4.4 μM was selected (i.e., evenly distributed through the bulk and surface layers of the snow crystal but obviously, nitrates were absent from the gas phase throughout the simulation).[3,10,16] When temperature-dependent rates were available, a temperature of 243 K (-30°C) was assumed.

I.B Bulk transport and (photo)chemistry:

Molecular transport kinetics for NO_2 (approximated herein using the diffusion coefficient for CO_2 in bulk ice at 243 K, D_{NO_2}, from Bereiter et al.)[13] and for nitrates ($D_{NO_3^-}$, calculated for T = 243 K using data from Thibert and Dominé)[12] were described using simple 1-D fickian diffusion.

The photolysis rate constant for nitrates in bulk ice, $J^{Bulk}_{NO_3^- photolysis}$, was taken from Galbavy et al.[4] In addition to the NO_2 (and O^-) photoproducts, nitrates photolysis in aqueous solutions is known to yield NO_2^- (and O) in proportions of 1 NO_2^- to 9 NO_2.[17] The minority nitrite photoproducts were treated as a net loss in the partial nitrogen budget of this model even though they may, as is the case in aqueous solutions,[1,2,17] undergo further photolysis (producing NO) or protonation (yielding HONO) in bulk ice or at its surface. While NO and HONO photoproducts are known to degas from ice under the conditions of the snowpack, thereby contributing to the total NO_x emissions to the interstitial air, HONO may also undergo secondary photolysis (yielding NO and OH) within ice, at its surface as well as in the gas phase.[1,2,17] These subsequent reaction pathways were not treated explicitly in the model.

Unfortunately, NO_2 hydrolysis rates in bulk ice, $k^{Bulk}_{NO_2\ hydrolysis}$, are unknown. In this model, NO_2 hydrolysis in bulk ice was assumed to proceed by a similar bimolecular reaction mechanism as reported by Cheung et al.[14] for NO_2 hydrolysis in aqueous solutions. Hydrolysis of NO_2 in aqueous solutions obeys second order kinetics with respect to $[NO_{2(aq)}]$ producing $HNO_{3(aq)}$ and $HONO_{(aq)}$. The reaction is relatively facile, occurring at a near diffusion-limited rate. As an approximation, it was therefore chosen to also treat the NO_2 hydrolysis rate constant as being diffusion-limited in bulk ice. The diffusion coefficient for CO_2 in bulk ice from Bereiter et al.[13] was thus used for self-consistency in order to provide an estimate of the NO_2 hydrolysis rate constant in bulk ice. In the model, $HNO_{3(aq)}$, a strong acid, is assumed to ionize spontaneously in bulk ice yielding nitrate anions (as well as excess protons). $HONO_{(aq)}$, a weak acid, is assumed to either rapidly

degas from ice, contributing to $HONO_{(g)}$ photochemical emissions to the snowpack interstitial air, or otherwise undergo secondary photolysis (either within ice, at its surface or in the gas phase) yielding NO and OH. As indicated above, neither NO, nor HONO emissions are treated explicitly in the model.

Soon after sunrise, the model reveals that as bulk nitrates photolysis builds up the NO_2 concentration in bulk ice (i.e., $t_{½}$ ~ 36.5 days for photolysis at the noon-time actinic flux), it reaches a quasi-stationary state with (the comparatively rapid) bulk NO_2 hydrolysis ($t_{½}$~2.6 h using the steady state noon-time bulk NO_2 concentrations). The NO_3^- (Figure S2A) and NO_2 (Figure S2B) concentrations (expressed as the number of molecules per layer) in layer 100 are displayed as they are representative of the bulk layers behavior. The bulk NO_2 concentration is seen to closely follow the modulations in actinic flux, while the bulk nitrates concentration displays oscillations that are, as expected, out of phase with the actinic flux (i.e., nitrates are photolyzed faster when the actinic flux is the highest). As discussed below, the effect of surface-enhanced nitrates photolysis are localised to the top 50 layers (i.e., ~80 nm) at the ice surface. Therefore, the bulk NO_3^- and NO_2 concentrations in layer 100 for simulations where the surface and bulk photolysis rates are equal ($k_s = k_b$; black traces) are identical (i.e., are superimposed in Figure S2A and S2B) to those where the photolysis rate is enhanced in the surface layer ($k_s = 3k_b$, red traces; $k_s = 6k_b$; green traces). While nitrates photolysis and NO_2 hydrolysis form a quasi-stationary state in the bulk, the bulk nitrates concentration slowly decays as a result of the minority photolysis channel, $NO_3^- \rightarrow NO_2^- + O$ (i.e., that displays ~0.1% photochemical quantum yield in ice), being treated as a net sink in the partial nitrogen budget of the model.

I.C Surface (photo)chemistry and $NO_{2(g)}$ emissions to the interstitial air:

Nitrates photolysis rates in the surface layer, $J^{Surface}_{NO_3^- photolysis}$, were either the same as those for the bulk (the photolysis rate constant reported by Galbavy et al.[4] were used: black traces, Figure S2), or they were increased 3x (red traces, Figure S2) or 6x (green traces, Figure S2) to account for enhanced nitrates photolysis at the surface of ice.

While homogeneous NO_2 hydrolysis is second order in $[NO_{2(aq)}]$ in bulk aqueous solutions, the kinetics for heterogeneous NO_2 hydrolysis were reported to be pseudo-first order with respect to $[NO_{2(g)}]$ and $[H_2O_{(g)}]$.[6,7] However, the nature of the aqueous medium whereupon the reaction takes place as well as the mechanism for heterogeneous NO_2 hydrolysis are complex and remain the subject of current debate.[7] For the purpose of the model, the heterogeneous NO_2 hydrolysis rates on ice were adapted from the temperature-dependent data of Svensson et al.[6] Specifically, the temperature dependence of the rate was interpreted as being due to variations in the probability of bimolecular reactive collisions of $NO_{2(g)}$ with $NO_{2(ads)}$ at the surface of ice and the rate thus extrapolated to 243 K using kinetic gas theory. Considering the reaction to be second order in $[NO_{2(ads)}]$, one estimates the effective bimolecular reaction rate constant to be 1.6×10^6 greater for NO_2 hydrolysis occurring in the surface layer than for the corresponding process occurring in the bulk layers (which was assumed to be diffusion limited; Section I.B). For comparison, enhancements in heterogeneous NO_2 hydrolysis as great as 10^5 were previously reported to occur in the presence of wet surfaces by Finlayson-Pitts et al.[7]

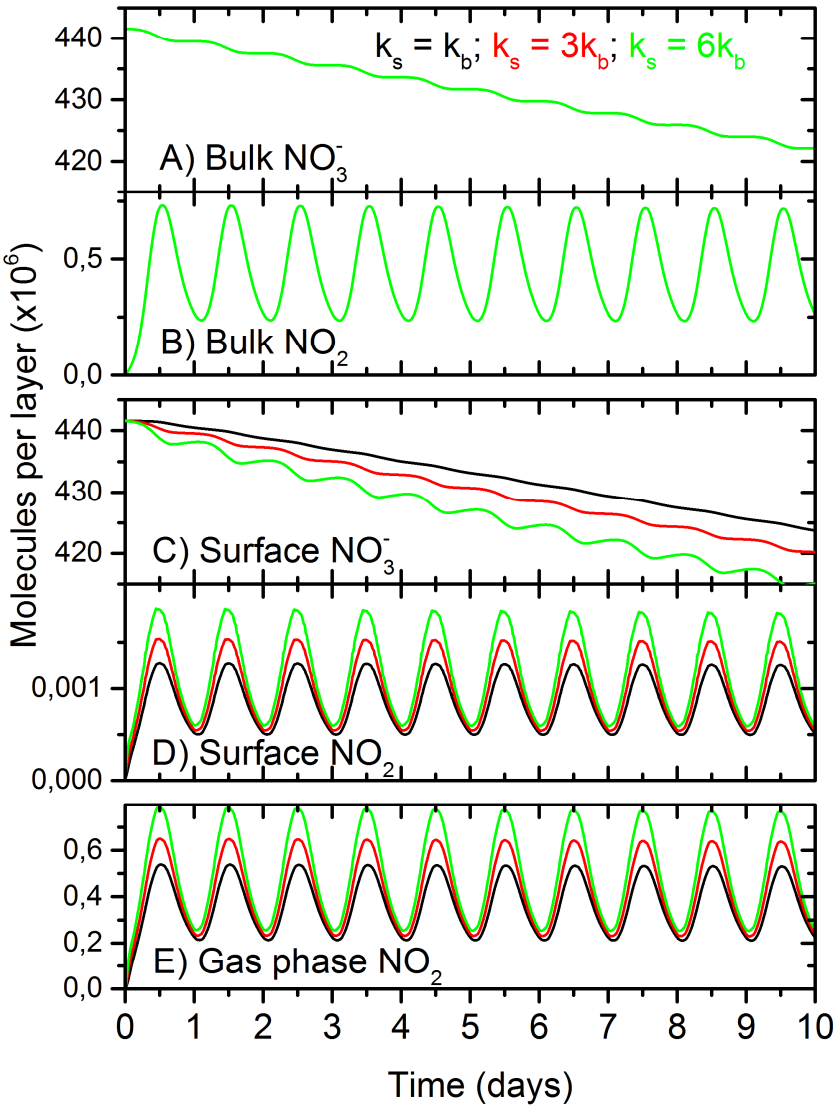

Fig. S2. Bulk NO_3^- (A) and bulk NO_2 (B) concentrations (expressed as the number of molecules in layer 100); surface NO_3^- (C) and surface NO_2 (D) concentrations (expressed as the number of molecules in layer 1); and gas phase NO_2 concentrations (E, expressed as the number of molecules in the gas phase) as a function of time. Simulation results where the surface and bulk nitrates photolysis rates are equal ($k_s = k_b$; black traces) are compared with simulation results where heterogeneous nitrates photolysis rates are enhanced three-fold (red traces, $k_s = 3k_b$) and six-fold (green traces, $k_s = 6k_b$) with respect to the bulk nitrates photolysis rates.

The adsorption/desorption equilibrium of NO_2 on ice was described using the gas/surface partition coefficient for NO_2 on the snowpack at 246 K, K_{ads}, proposed by Bartels-Rausch et al.[9] which were scaled to the surface-to-volume ratio of the model. Finally, as for the bulk layers, diffusion of NO_2 and NO_3^- in and out of the surface layer were described using simple 1-D fickian diffusion.

Whereas the bulk NO_3^- (Figure S2A) and NO_2 (Figure S2B) concentrations are identical for simulations where the surface and bulk photolysis rates are equal to those where the photolysis rate is enhanced 3(6)-fold in the surface layer, the surface NO_3^- (Figure S2C) and surface NO_2 (Figure S2D) concentrations are quite sensitive to the effects of enhanced surface nitrates photolysis. According to expectations from an enhancement in heterogeneous NO_3^- photolysis rates, the surface NO_3^- concentration (Figure S2C) decreases more rapidly as a result of the 3(6)-fold enhancement in heterogeneous nitrates photolysis ($k_s = 3k_b$, red trace; $k_s = 6k_b$, green trace) compared to simulations where the surface and bulk photolysis rates are equal ($k_s = k_b$, black trace). Furthermore, the amplitude in the diurnal modulations in NO_3^- and NO_2 concentration in the surface layer increases as a result of a 3(6)-fold enhancement in heterogeneous nitrates photolysis rate. Most interestingly however, the concentration of NO_2 in the topmost surface layer on ice (Figure S2D) remains ~500 times smaller than that in bulk ice (Figure S2B) throughout the simulation. This very small NO_2 concentrations in the surface layer results from the efficient NO_2 sinks provided by rapid heterogeneous NO_2 hydrolysis and desorption to the gas phase. Nevertheless, a three-fold enhancement (i.e., the average enhancement in effective photolysis rates with contributions from all the distorted geometries of nitrates adsorbed onto ASW) yields a 30% increase in direct photochemical NO_2 emissions as can be gleaned from the increase in amplitude of the diurnal oscillations in interstitial air $NO_{2(g)}$ concentration (i.e., red trace, Figure S2E). A six-fold enhancement in photolysis rates (i.e., as that displayed by the most distorted nitrates, that is those that display a >200 cm^{-1} gap in their asym-$NO_{str.}$ splitting) results in a 60% increase in NO_2 emissions (i.e., green trace, Figure S2E). Therefore, despite the relatively small 1:2999 surface to volume ratio used in the model, the photochemical NO_2 emissions arising from surface nitrates photolysis (i.e., nitrates in the top-most molecular layer on ice) contribute greatly to the total NO_2 emissions (i.e., 30%(60%) for 3x(6x) enhancements in surface photolysis rates). At first sight, these enhancements may seem rather modest however, if all 2999 bulk layers contributed to the photochemical NO_2 flux, one should have expected an enhancement in NO_2 emissions of the order 3002/3000=1.0007 (3005/3000=1.0017) for a 3x(6x)enhancement in surface photolysis rates, that is a mere 0.07%(0.17%). The observation reported herein could therefore be argued to represent more than a two orders of magnitude relative increase in the contribution of the surface layer to photochemical NO_2 emissions.

The complex and strongly coupled transport (i.e., adsorption/desorption/diffusive uptake) and reactions (i.e., photolysis/hydrolysis) kinetics rapidly establish a quasi-stationary state in the surface layer. Detailed analysis of this quasi-stationary state is provided by inspection of the various individual contributions to the changes in NO_2 concentrations in the surface layer (expressed as the change in the number of NO_2 molecules in the surface layer) due to each of the elementary processes for individual time steps along the simulation as reported in Figure S3. For all three simulations [i.e., those without surface enhancement (Figure S3A, $k_s = k_b$) as well as those with 3-fold (Figure S3B, $k_s = 3k_b$) and 6-fold (Figure S3C, $k_s = 6k_b$) surface-enhanced nitrates photolysis rates], the dominant sources of NO_2 to the surface layer arise from nitrates photolysis (blue trace) and NO_2 diffusion from the bulk layers (red trace).

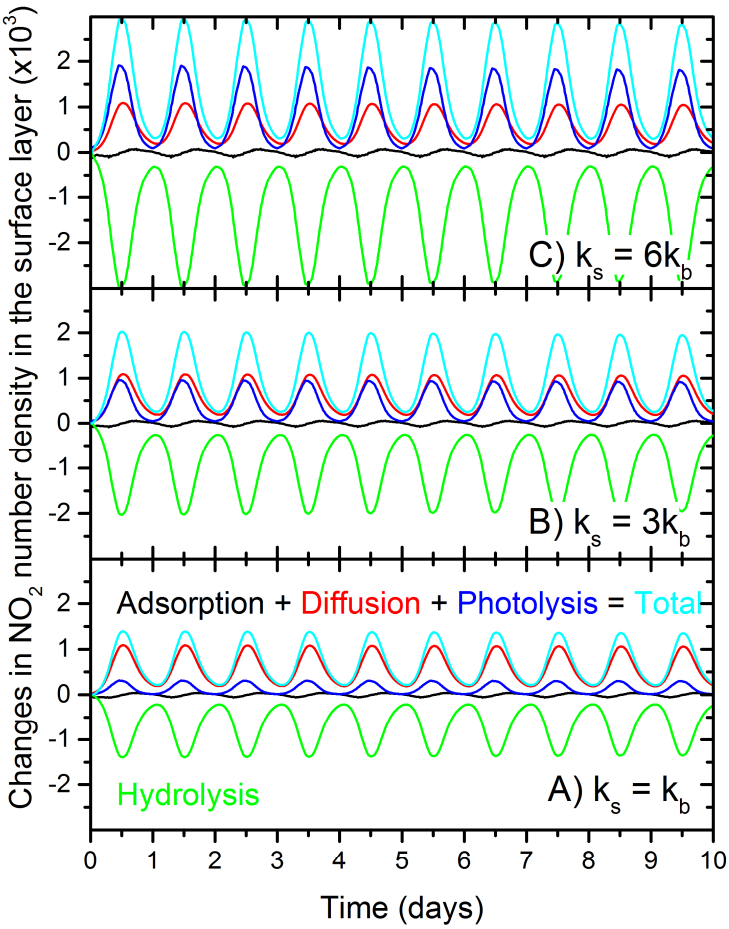

Fig. S3. Contributions to the changes in NO_2 concentrations (i.e., number density in cm^{-2}) in the surface layer (i.e., layer 1) from the individual elementary processes: adsorption/desorption from the gas phase (black trace), diffusion from bulk ice (red trace), nitrates photolysis (blue trace) and NO_2 hydrolysis (light green trace). The total contribution of all sources of NO_2 to the surface layer (Adsorption+Diffusion+Photolysis = Total; cyan trace) for the three cases [i.e., A) $k_s = k_b$: no surface enhancement; B) $k_s = 3k_b$: three-fold surface enhancement; and C) $k_s = 6k_b$: six-fold surface enhancement] creates a quasi-stationary state with heterogeneous NO_2 hydrolysis (light green trace), the dominant sink for NO_2 in the surface layer.

However, NO_2 molecules arising from photolysis or diffusing to the surface layer are efficiently converted back to nitrates by heterogeneous NO_2 hydrolysis (green trace). Indeed, the heterogeneous NO_2 hydrolysis rate constant is greatly enhanced with respect to that of the bulk (i.e., by a factor of 1.6×10^6 if one chooses to compare the diffusion-limited bulk hydrolysis rate constant with an effective second order rate constant for bimolecular adsorbed NO_2 hydrolysis: $k_{eff}[NO_{2(ads)}]^2$). The resulting average effective NO_2 hydrolysis rates in the surface layer (arithmetic mean between the maximal daytime and the minimal nighttime hydrolysis rates) are enhanced ~7.5 fold with respect to the bulk NO_2 hydrolysis

rates (i.e., this enhancement in the rate is much smaller than the enhancement in rate constant due to the ~500-fold smaller surface NO_2 concentration, displayed in Figure S2D, compared to the bulk NO_2 concentration, displayed in Figure S2B). Overall, the contribution from NO_2 adsorption/desorption to the NO_2 concentration in the surface layer (black traces in Figure S3A, S3B and S3C) remains small throughout the simulation and is lagging behind the diffusive and photochemical fluxes by about six hours.

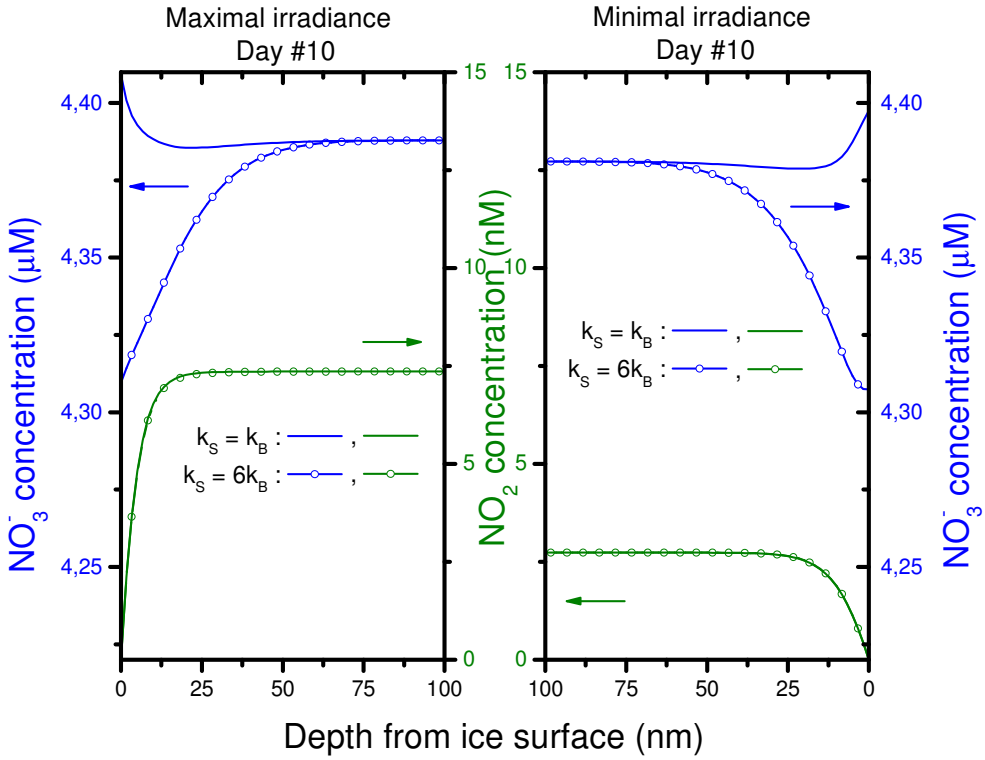

Fig. S4. Instantaneous concentration profiles for NO_3^- (blue traces) and NO_2 (green traces) as a function of depth within the ice crystal upon maximal (noon, left panel) and minimal (midnight, right panel) irradiance conditions on day #10 of the simulation. The concentration profiles where the surface and bulk photolysis rates are identical ($k_s = k_b$) are displayed as continuous lines without symbols while those where a six-fold enhancement in surface photolysis rates with respect to the bulk ($k_s = 6k_b$) is imposed are displayed as continuous lines with symbols (○).

Further insight into the complex coupled interfacial kinetics is provided by analysis of the concentration profiles in the near-surface region of the ice. In Figure S4, the maximal irradiance (day #10 at noon; left panel) and minimal irradiance (day #10 at midnight; right panel) concentration profiles for NO_2 (green traces) and NO_3^- (blue traces) provided by the model are compared. Simulation results where the surface and bulk photolysis rates are identical ($k_s = k_b$) are reported as continuous lines without symbols while those where the surface rates are enhanced six-fold ($k_s = 6k_b$) are reported as continuous lines with symbol (○). In agreement with Figure S2A and S2B, model results show that, in the bulk, the effects of enhanced heterogeneous nitrates photolysis are negligible. Indeed, the bulk NO_2 concentrations remain uniform until it reaches the top 15 ice layers [i.e., the effects of the

surface enhanced hydrolysis and photolysis rates do not reach deeper than ~25 nm from the surface]. While the diurnal cycles in the actinic flux causes the bulk NO_2 concentration to exhibit oscillations (i.e., see Figure S2B) between peak concentrations near noon and minimum concentrations near midnight as a result of the (photo)chemical quasi-stationary state between bulk nitrates photolysis and bulk NO_2 hydrolysis, the NO_2 concentrations in the surface layer always remain ~500-fold smaller than the bulk concentrations (i.e., see Figure S2B and S2D) as a result of the rapid NO_2 desorption and heterogeneous hydrolysis.

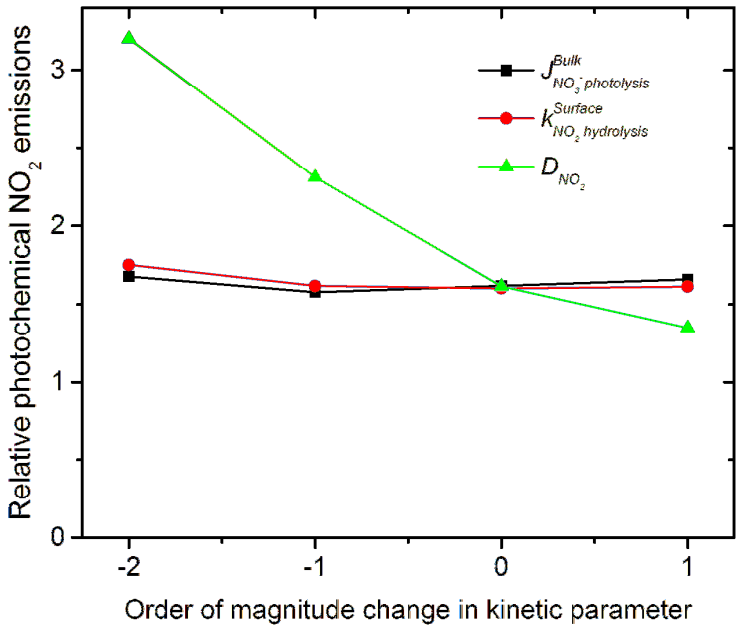

Fig. S5. Results of a sensitivity analysis highlighting the effects of a few orders of magnitude changes in the most poorly constrained kinetic parameters of the model: the bulk nitrates photolysis rate constant (using a fixed 6x enhancement in surface nitrates photolysis - black symbols), the heterogeneous NO_2 hydrolysis rate constant (red symbols), as well as the bulk NO_2 diffusion coefficient (along with the corresponding bulk NO_2 hydrolysis rate constant - green symbols).

As several of the kinetic parameters used in the model are poorly constrained, a detailed sensitivity analysis was performed to demonstrate that these phenomena (i.e., the increased photochemical NO_2 emission and formation of a photochemically active layer) are robust with respect to changes in bulk nitrates photolysis rates, in bulk NO_2 diffusion coefficient, as well as to changes in heterogeneous NO_2 hydrolysis rates, over several orders of magnitude. Changing bulk nitrates photolysis rates, while maintaining the 6x enhancement in nitrates photolysis at the surface of ice, has very little effect on the relative increase in NO_2 emissions (Figure S5, black squares). Indeed, while the amplitude of the NO_2 emissions vary strongly with bulk nitrates photolysis rates, the relative increase in photochemical NO_2 emissions remain more or less constant at ~60% for a fixed 6x

enhancement in surface photolysis rate despite a few orders of magnitudes changes in bulk nitrates photolysis rates. The increase in NO_2 emissions due to enhanced surface nitrates photolysis also appears rather insensitive to a few orders of magnitude changes in the heterogeneous NO_2 hydrolysis rate (Figure S5, red circles), as long as it remains sufficiently fast to maintain a strong NO_2 concentration gradient in the photochemically active layer. However, the sensitivity of the increase in NO_2 emissions to the bulk NO_2 diffusion coefficient in ice is more pronounced (Figure S5, green triangles). As this latter controls both the bulk transport kinetics for NO_2 as well as the bulk NO_2 hydrolysis rate, using a smaller diffusion coefficient for NO_2 further increases the NO_2 emissions due to enhanced heterogeneous nitrates photolysis by reducing the thickness of the photochemically active layer which further amplifies the effects of the 6x enhancement in heterogeneous nitrates photolysis. In summary, the magnitude of the enhancement due to enhanced heterogeneous nitrates photolysis, the thickness of the photochemically active layer, and the relative contributions of the fast direct photochemical emissions to the slow diffusive NO_2 release depend somewhat on the kinetic parameters that are employed. Nevertheless, this rudimentary model highlights the fact that contributions from the distinctive character of interfacial reaction dynamics on ice should contribute very significantly to the total NO_2 emissions.

II. References:

(1) Thomas, J. L.; Stutz, J.; Lefer, B.; Huey, L. G.; Toyota, K.; Dibb, J. E.; von Glasow, R. Modeling Chemistry in and above Snow at Summit, Greenland – Part 1: Model Description and Results. *Atmos. Chem. Phys.* **2011**, *11*, 4899–4914.

(2) Boxe, C. S.; Saiz-Lopez, A. Multiphase Modeling of Nitrate Photochemistry in the Quasi-Liquid Layer (QLL): Implications for NO_x Release from the Arctic and Coastal Antarctic Snowpack. *Atmos. Chem. Phys. Discuss.* **2008**, *8*, 6009–6034.

(3) Honrath, R. E.; Lu, Y.; Peterson, M. C.; Dibb, J. E.; Arsenault, M. A.; Cullen, N. J.; Steffen, K. Vertical Fluxes of NO X ; HONO , and HNO3 above the Snowpack at Summit , Greenland. *Atmos. Environ.* **2002**, *36*, 2629–2640.

(4) Galbavy, E. S.; Anastasio, C.; Lefer, B. L.; Hall, S. R. Light Penetration in the Snowpack at Summit, Greenland: Part 1. *Atmos. Environ.* **2007**, *41*, 5077–5090.

(5) Krepelová, A.; Newberg, J.; Huthwelker, T.; Bluhm, H.; Ammann, M. The Nature of Nitrate at the Ice Surface Studied by XPS and NEXAFS. *Phys. Chem. Chem. Phys.* **2010**, *12*, 8870–8880.

(6) Svensson, R.; Ljungstrom, E.; Lindqvist, O. Kinetics of the Reaction between Nitrogen Dioxide and Water Vapour. *Atmos. Environ.* **1987**, *21*, 1529–1539.

(7) Finlayson-Pitts, B. J.; Wingen, L. M.; Sumner, A. L.; Syomin, D.; Ramazan, K. A. The Heterogeneous Hydrolysis of NO_2 in Laboratory Systems and in Outdoor and Indoor Atmospheres: An Integrated Mechanism. *Phys. Chem. Chem. Phys.* **2003**, *5*, 223–242.

(8) King, M. D.; Simpson, W. R. Extinction of UV Radiation in Arctic Snow at Alert, Canada (82°N). *J. Geophys. Res.* **2001**, *106*, 12,499–12,507.

(9) Bartels-Rausch, T.; Eichler, B.; Zimmermann, P.; Ammann, M. The Adsorption Enthalpy of Nitrogen Oxides on Crystalline Ice. *Atmos. Chem. Phys.* **2002**, *2*, 235–247.

(10) Dibb, J. E.; Arsenault, M.; Peterson, M. C.; Honrath, R. E. Fast Nitrogen Oxide Photochemistry in Summit, Greenland Snow. *Atmos. Environ.* **2002**, *36*, 2501–2511.

(11) Frey, M. M.; Brough, N.; France, J. L.; Anderson, P. S.; Traulle, O.; King, M. D.; Jones, A. E.; Wolff, E. W.; Savarino, J. The Diurnal Variability of Atmospheric Nitrogen Oxides (NO and NO_2) above the Antarctic Plateau Driven by Atmospheric Stability and Snow Emissions. *Atmos. Chem. Phys.* **2013**, *13*, 3045–3062.

(12) Thibert, E.; Domine, F. Thermodynamics and Kinetics of the Solid Solution of HNO_3 in Ice. *J. Phys. Chem. B* **1998**, *102*, 4432–4439.

(13) Bereiter, B.; Schwander, J.; Lüthi, D.; Stocker, T. F. Change in CO_2 Concentration and O_2/N_2 Ratio in Ice Cores due to Molecular Diffusion. *Geophys. Res. Lett.* **2009**, *36*, L05703.

(14) Cheung, J. L.; Li, Y. Q.; Boniface, J.; Shi, Q.; Davidovits, P.; Worsnop, D. R.; Jayne, J. T.; Kolb, C. E. Heterogeneous Interactions of NO_2 with Aqueous Surfaces. *J. Phys. Chem. A* **2000**, *104*, 2655–2662.

(15) Domine, F.; Albert, M.; Huthwelker, T.; Jacobi, H.-W.; Kokhanovsky, A. A.; Lehning, M.; Picard, G.; Simpson, W. R. Snow Physics as Relevant to Snow Photochemistry. *Atmos. Chem. Phys. Discuss.* **2008**, *8*, 171–208.

(16) Jones, A. E.; Weller, R.; Wolff, E. W.; Jacobi, H.-W. Speciation and Rate of Photochemical NO and NO_2 Production in Antarctic Snow. *Geophys. Res. Lett.* **2000**, *27*, 345–348.

(17) Mack, J.; Bolton, J. R. Photochemistry of Nitrite and Nitrate in Aqueous Solution : A Review. *J. Photochem. Photobiol. A Chem.* **1999**, *128*, 1–13.